J Mater Sci (2006) 41:5882–5889
DOI 10.1007/s10853-006-0262-x

Shear induced phase coarsening in Polystyrene/Styrene-ethylene-butylene-styrene blends

Yong Wang · Cong Wang · Qin Zhang ·
Hong Yang · Rongni Du · Qiang Fu

Received: 10 March 2005 / Accepted: 13 October 2005 / Published online: 6 July 2006

Abstract The phase behavior of polymer blends under the effect of shear has been a subject of considerable interest from the viewpoint of both theoretical research and industrial application, because the shear stress is unavoidable during processing. In this work, we reported the change of phase behavior and mechanical properties of Polystyrene (PS)/Styrene-ethylene-butylene-styrene (SEBS) blends achieved via a shear-assistant injection molding, which was called dynamic packing injection molding (DPIM). The size of dispersed SEBS particles in PS matrix was found to be increased for the samples obtained by dynamic packing injection molding (DPIM), compared with those obtained by conventional molding, indicating a shear induced phase coarsening. The shear induced phase coarsening can be further demonstrated by the decrease of impact strength of dynamic packing injection molded samples. However, the shear-induced phase coarsening will be eliminated after annealing the samples at high temperature for certain time. The particle size, which related to the capability to deform under the effect of shear, was found to play an important role to determine the phase morphology. Our result suggested that shear stress induced phase coarsening was a process of not only molecular configuration change but also deformation change under shear.

Y. Wang · C. Wang · Q. Zhang · H. Yang · R. Du · Q. Fu (✉)
Department of Polymer Science and Materials, Sichuan University, State Key Laboratory of Polymer Materials Engineering, No.24, 1st southsection, yihuan Road, Chengdu, Sichuan 610065, China
e-mail: qiangfu@scu.edu.cn

Y. Wang
College of Materials Science and Engineering, Southwest Jiaotong University, Chengdu 610031, China

Introduction

The phase behavior of polymer blends under the effect of shear has been a subject of considerable interest from the viewpoint of both theoretical research and industrial application, because the shear stress is unavoidable during processing. Shear-induced phase miscible or separation in polymer blends is a relative new phenomenon [1–4]. Owing to the relative ease in experimental observation of shear effect on polymer solutions, a lot of work has been done on polymer solutions, and this has been comprehensively reviewed by Rangel-Nafail [5] and Hindawi [6]. For polymer melt blends, however, the phase behavior under shear flow is as yet unexplored both experimentally and theoretically, and remains a challenging area of research. The data collected for some polymer blends show that shear flow greatly affects miscibility in polymer blends and shear rates of less than 1 s^{-1} are sufficient to induce changes in the phase behavior [7, 8]. Shear-induced LCST (lower critical solution temperature) depression and elevation have been observed in several systems [9, 10]. In a study of polypropylene/high density polyethylene (PP/HDPE) blends, Inoue and coworkers proposed a single-phase mixture of PP/HDPE = 60/40 obtained in high shear fields in an injection machine based on the regularly phase-separated structure [11]. A bi-continuous two-phase structure, with unique periodicity was shown to develop by a dissolution caused by LCST elevation under high shear rate from a nozzle, and then spinodal decomposition under zero shear rate after the melt was injected into a mold. Similar structure development was seen for injection molding of a 50/50 polycarbonate (PC)/AS blend [12] and 50/50 linear low-density polyethylene/polypropylene (LLDPE/PP) blend [13]. Interestingly, the co-continuous phase structure in LLDPE/PP was found to be broken down to sea-island like structure when a low shear rate was applied via dynamic packing injection molding or simply by manually deforming the static samples [13]. Furthermore, the temperature was found to be one of the important factors that determined the phase behavior in the shear stress field. Fernandez [14] found that shear induced phase coarsening at a lower initial shear temperature below the quiescent LCST, while shear induced miscible was observed at a higher initial shear temperature but below the quiescent LCST. The effect of shear fields on phase behavior is theoretically interpreted in terms of the enhancement of concentration fluctuations and the elastic contribution to the free energy of mixing, resulting in a ''shift'' of the phase boundary of a polymer blends. So far, almost all the literatures deal with the effect of shear on the phase behavior of polymer blend by using a rheo-optical light scattering device [15–18], no associated change of mechanical properties has been reported.

Due to the similar structure of styrene block, SEBS is widely used as toughening agent for polystyrene (PS) [19]. In this work, the effect of shear stress on phase behavior and associated change of mechanical properties of PS/SEBS blends were investigated through so called dynamic packing injection molding (DPIM), which relies on the application of shear stress fields to melt/solid interfaces during the packing stage by means of hydraulically actuated pistons. Thus a low shear rate is produced in this way during the solidification process. The pioneering work of this technology began on 1986, when Prof. Bevis reported such technology and owned the patent [20]. And then much work has been done on different polymer materials [21–26]. The main feature is that after the melt is injected into the mold the specimen is forced to move repeatedly in a chamber by two pistons that move reversibly with the same frequency as the solidification progressively occurs from the mold wall to the molding core part. The phase morphology and related mechanical properties of samples obtained were characterized by SEM, DSC and mechanical testing. Our result showed an enhanced phase coarsening by a low shear rate in PS/SEBS blends, accompanied by a deterioration of mechanical properties.

Experimental

Materials

The polystyrene (PS) and SEBS used in the experiment were commercial products, PS (666D, melt flow rate is 4.3 g/10 min) was purchased from the Yan Shan Petroleum Chemical, China; and SEBS was purchased from Ba Ling Petroleum Chemical, China. In order to study the effect of SEBS structure, two kinds of SEBS (i.e., linear and star) were used. The detailed information of materials used in the experiment was shown in Table 1. SBS was also used for comparison and its parameters are included in Table 1.

Table 1 Properties of materials

Materials	Trademark	Molecular weight	PS%	Company
PS	666D	54,000	100	Yan Shan Petrol. Chem., China
SBS	1401-1	100,000	40	Yan Shan Petrol. Chem., China
SEBS	502	110,000	30	Ba Lin Petrol. Chem., China
SEBS	602	240,000	40	Ba Lin Petrol. Chem., China

Samples preparation

Melt blending of PS/SEBS was conducted by using twin-screw extruder (TSSJ-25 co-rotating twin-screw extruder) set at a barrel temperature of 180–210°C. After making droplets, the blends were injected into a mold of 3.5 mm in thickness and 6 mm in width, using SZ 100 g injection molding machine set at the temperature of 180°C and the injection pressure of 90 MPa. For the sample of pure PS, although it was not extruded by twin-screw extruder, it was injected and molded in the same fashion as others. Then dynamic packing injection molding technology was applied. The main feature was that the specimen was forced to move repeatedly in a chamber by two pistons that moved reversibly with the same frequency as the solidification progressively occurred from the mold wall to the molding core part. The shear rate was about 10 s^{-1} calculated from the geometry of the mold. The schematic representation of this method can be seen in Fig. 1, the moving directions of these two pistons were shown as the arrows. One moves in while the other one moves out. The processing parameters can be found somewhere in the literatures [27]. The cycle times and temperatures keep constant with the change of composition. This procedure is similar to the model ''short term'' shear experiments devised by Janeschitz-Kriegl and coworkers [28]. The difference is that in our experiment the shear time (3 s) is periodical and through this method not only morphology but also mechanical properties can be investigated at the same time. We also carried out injection molding under static packing by using the same processing parameters without shearing for comparison purpose. The specimen obtained by dynamic packing injection molding is called dynamic sample, and the specimen obtained by static packing injection molding is called static sample. The processing parameters are listed in Table 2.

For static samples, skin-core morphology is usually observed. For dynamic samples, the shear-induced

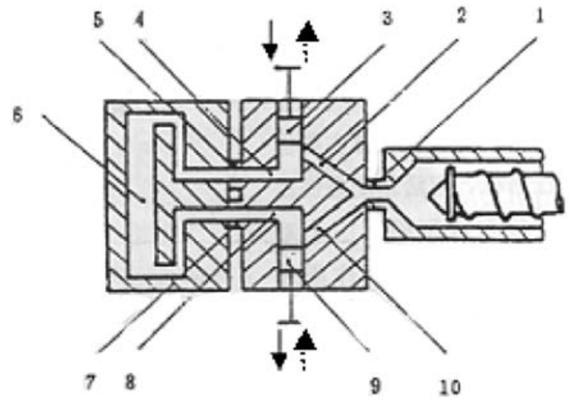

Fig. 1 The schematic representation of dynamic packing injection molding, and the arrows show the moving direction of pistons. (1) Nozzle, (2) sprue A, (3) piston A, (4) runner A, (5) connector, (6) specimen, (7) connector, (8) runner B, (9) piston B, (10) sprue B

Table 2 Processing parameters of dynamic packing injection molding technology

Processing parameters	Parameters value
Injection pressure (MPa)	90
Packing pressure (MPa)	50
Melt temperature (°C)	180
Dynamic packing pressure (MPa)	35
Dynamic packing frequency(Hz)	0.3

morphologies with core in the center and oriented zone surrounding the core are observed in the cross-section areas of the samples. The DSC and SEM experiment were carried out, by using the core layer for static samples and the oriented layers for dynamic samples, respectively.

Differential scanning calorimetry (DSC)

In a differential scanning calorimeter (Perkin-Elmer DSC priys-1), the heating of slices cut from the same place in both static samples and dynamic samples of PS/SEBS blends were characterized at a scanning rate of 10 °C /min in nitrogen atmosphere.

Scanning electronic micrograph (SEM) experiment

The morphologies of the blends were studied by preferential etching of the elastomers phase in *n*-heptane for 2 h at the temperature of 20 °C. The samples were fractured in liquid nitrogen prior to etching. The exposure of the sample to hexane for 2 h may soften PS matrix for certain degree, and TEM is needed on stained sample by certain heavy-metal stains that will differentiate between these two materials. Then the phase morphology was observed in an SEM instrument, JSM-5900LV, operating at 20 kV. In order to assure the consistent result, the same regions of all the samples, including static and dynamic samples, were selected during the SEM experiment.

Mechanical properties measurement

The sketch of mechanical test specimen dimensions according to the ASTM 638M standard can be seen in our other work [21], the length of the specimen is 112 mm and the width of sample is 6 mm. Shimadzu AG-10TA Universal Testing Machine was used to get the tensile strength according to GB/1040-92 standard method; the moving speed was 50 mm/min, and the measure temperature was 20 °C. For impact strength measurement, a notch with 45° was made by machine and remained width was 5.0 mm.The experiment was carried out on an I200XJU-2.75 Impact tester according to ISO 179. The values of all the mechanical parameters were calculated as averages over six to nine specimens for each composition.

Results

SEM results

The evidence of shear-induced phase coarsening comes directly from the SEM results, as shown in Fig. 2. Fig. 2a is the change of the morphology for PS/SEBS static samples at central part (the core) as a function of composition up to 40wt% SEBS. The black domains indicate the position of the extracted SEBS phases. One observes a sea-island structure in the composition investigated, which indicates that SEBS forms a dispersed phase and PS forms a continuous phase. Fig. 2b shows the morphological change as a function of SEBS content for PS/SEBS blends of dynamic samples, by which the effect of shear stress on the phase behavior can be demonstrated. Compared Fig. 2b with Fig. 2a, one observes an obvious increase of domain size of SEBS under the effect of shear stress. From 10 to 40wt% of SEBS content, the size of SEBS increases from 0.4–0.5 micron of static samples to 0.5–2.0 micron of dynamic samples. So SEM result shows a much-increased SEBS phase domain under the effect of shear, especially for samples with high SEBS content, which indeed suggests a shear-induced phase coarsening.

If the observed phase coarsening is induced by shear for dynamic samples, one should see the change of phase morphology after annealing the sample at high temperature. Shown as an example, the comparison of the morphologies of PS/SEBS (80/20) dynamic samples before and after annealing are shown in Fig. 3. The dynamic sample was annealed at the temperature of 100 °C, and

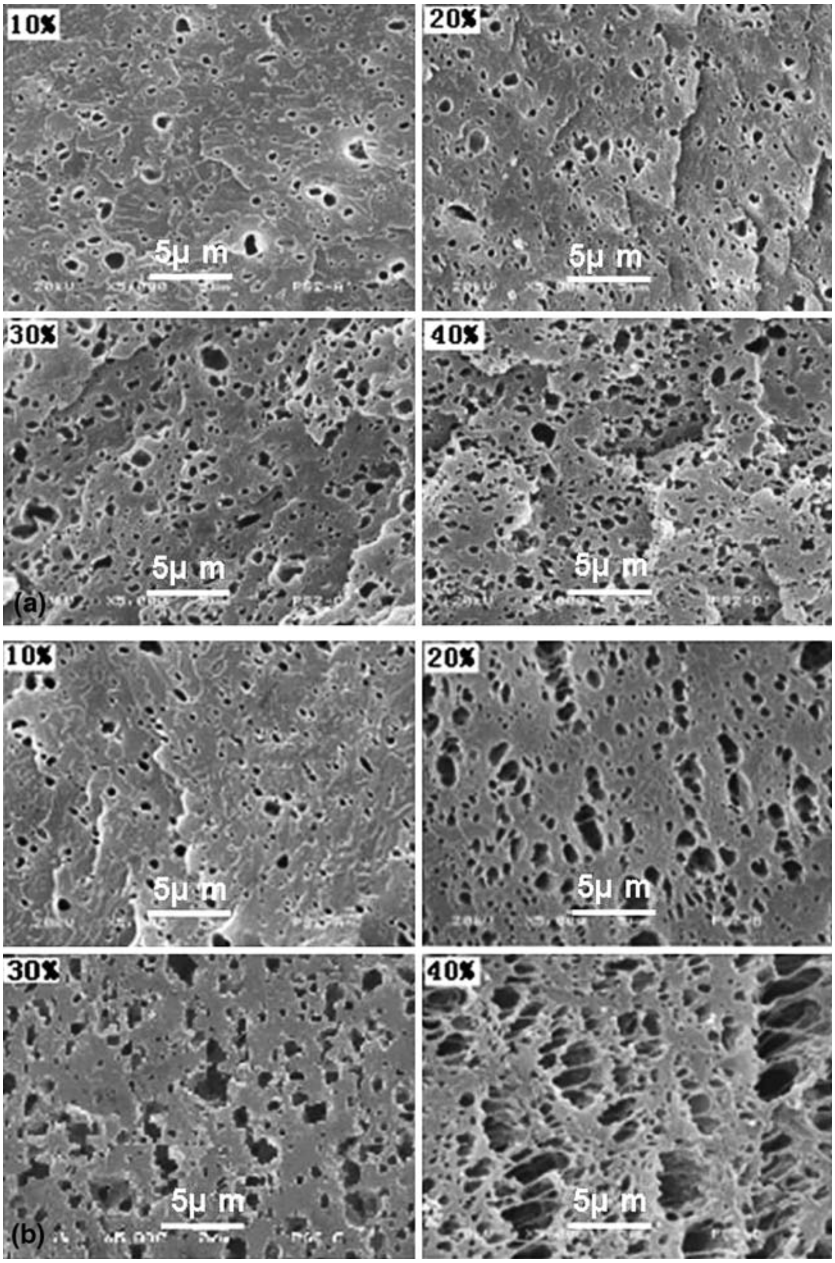

Fig. 2 The morphology comparison as the function of SEBS content between static samples and dynamic samples. The numbers in the photographs represent the weight fraction of SEBS in the blends. (a) static samples and (b) dynamic samples

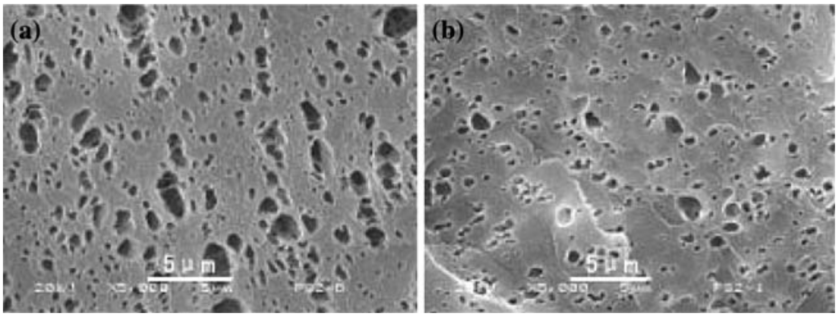

Fig. 3 The morphology comparison of dynamic samples PS/SEBS (80/20) before and after annealing. (a) before annealing and (b) after annealing

the duration time was about 4 h. It can be seen that, after annealing, the dispersed particles become homogeneous and the particle size decrease greatly. Furthermore, the morphology of dynamic samples after annealing for 4 h is almost the same with the static samples (Seen Fig. 2), which suggests that the effect of shear stress on phase

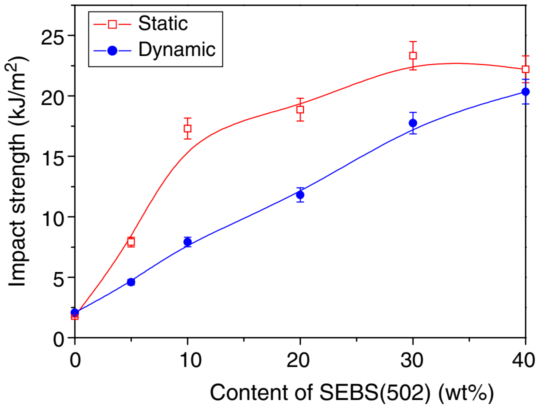

Fig. 4 The impact strength of PS/SEBS blends as the function of SEBS content

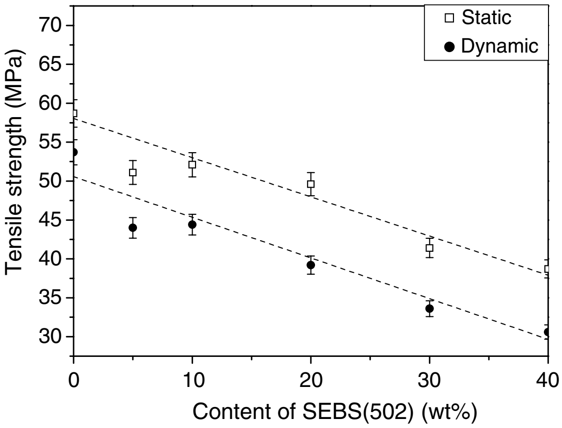

Fig. 5 The tensile strength of PS/SEBS blends as the function of SEBS content

morphology can be eliminated and the blends go back to their initial state (without effect of shear). Future work is needed to further verify the annealing effect is not due to the dissolution of the SEBS in the PS matrix at 100 °C.

Mechanical properties

It is well known that the morphology and phase behavior of polymer blends determine the mechanical properties, such as the impact strength and tensile strength. So, the effect of shear stress on the mechanical properties is one of the interesting topics. Figure 4 shows the impact strength of PS/SEBS blends obtained by both static and dynamic packing injection molding. For static samples, it can be seen that the impact strength increases with the increasing of SEBS content. The impact strength shows a rapid increase as SEBS content increases to 10 wt%, then increase slowly when SEBS content varies from 20 wt% to 40 wt%, which is in agreement with the literature. For the dynamic samples, however, one observes much-reduced impact strength and a linear relationship between impact strength and SEBS content is seen, which indicates a difference of toughening mechanism between static samples and dynamic samples. The reduced impact strength of PS/SEBS blends can be well understood as resulting from the increased phase coarsening under effect of shear. Some change of molecular orientation of PS or internal stress induced by shear may also contribute to the change of impact strength. But these effects should be negligible because PS chain is very difficult to be oriented due to its rigid structure, and the internal stress may only affect the tensile strength (see below), but not much impact strength of PS. One observes no difference of impact strength between static and dynamic samples for pure PS. Figure 5 shows the change of tensile strength as increase of SEBS content for static and dynamic samples. It can be seen that the tensile strength linearly decreases with the increasing of SBS content, which is consistent with the results observed in the documents, and the tensile strength of dynamic samples is smaller than that of static samples for all the composition studied. Since the difference of tensile

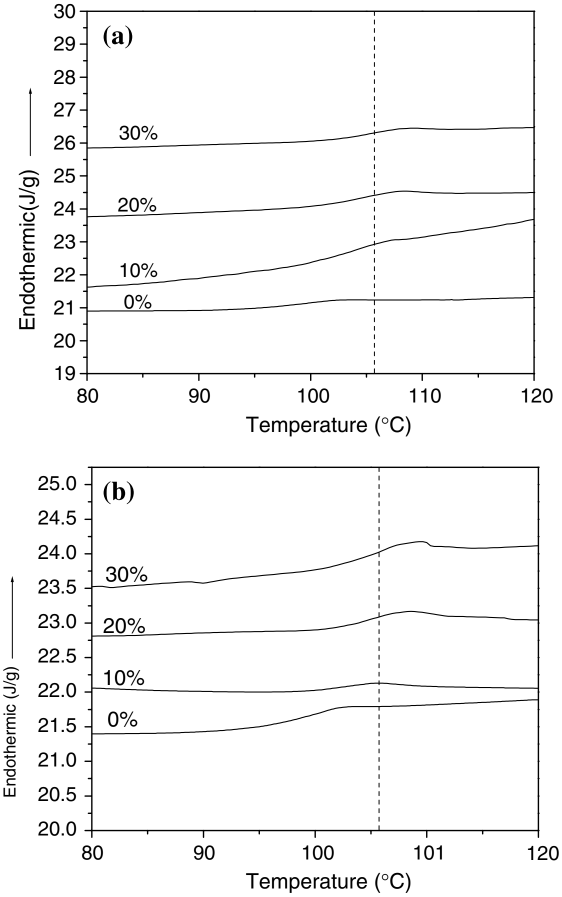

Fig. 6 The glass transition (T_g) of PS/SEBS obtained via DSC. (a) static samples and (b) dynamic samples, and the numbers show the content of SEBS. SEBS% = 1:0%, 2:10%, 3:20%, 4:30%

strength between static and dynamic samples keeps constant at all the composition studied including pure PS, the reduced tensile strength should not be considered as due to the shear induced phase coarsening, but most likely due to the increased internal stress induced by shear.

DSC result

One may expect a similar glass transition temperature of PS between the static and dynamic samples because the phase separated morphology. To prove this, the DSC experiment was carried out to measure the glass transition temperature (T_g). This is shown in Fig. 6. The T_g of PS shows a slightly increase by adding SEBS for both static and dynamic samples. But there is not much difference of T_g between the static and dynamic samples. Since SEBS itself has a multi-phase structure, the slight increase of T_g of PS, instead of decrease by adding SEBS, can be explained as the confined PS chains after adding SEBS.

Discussion

Here again, our work shows a good example that how the phase morphology and mechanical properties of a polymer blend could be affected by shear stress. More importantly, one observes an associated change of impact strength of PS/SEBS blends. To understand the shear-induced morphological change, one should recall the Horst and Wolf's prediction [29–31], in which an item of elastic energy was introduced stemming from the molecular configuration change under shear field into the Flory–Huggins mean field theory. The phase diagram of a binary polymer blend under the shear field could be described as following:

$$\frac{\partial^2 \Delta G_\gamma / RT}{\partial \Phi_2^2} = \frac{\partial^2 \Delta G_{\mathrm{eq}} / RT}{\partial \Phi_2^2} + \frac{\partial^2 E_{\mathrm{s}} / RT}{\partial \Phi_2^2} \tag{1}$$

Here, ΔG_γ is a generalized Gibbs energy, ΔG_{eq} is a Gibbs energy of mixing (zero shear, equilibrium condition) and E_{s}, the energy a system can story in the stationary state while it flows, Φ_2 is the volume fraction of polymer, T is the temperature and R, a constant. In our system, however, the deformation or breakup of droplets of the dispersed phase may also play a big role to determine the final phase morphology. Katsaros [32] had proved that it was possible that any small changes in the probability that groups might come together and form specific interactions could significantly alter the phase behavior of the polymer blends; Similarly, if any of the blend components were stretched and oriented, the entropy of mixing would be reduced, which was unfavorable to mix, and then resulting in the phase coarsening. It is well known that the morphology of polymer blends depends mainly upon the rheological and interfacial properties, the blending conditions, and the volume ratio of the components. The size and the deformation of a purely viscous (Newtonian) particle surrounded by another Newtonian fluid is determined mainly by two parameters [33–34]: the viscosity ratio (λ):

$$\lambda = {}^{\eta_{\mathrm{d}}}\!/_{\eta_{\mathrm{m}}} \tag{2}$$

In the equation, the η_{d} is the viscosity of dispersed phase and the η_{m} is the viscosity of matrix.

(a) The capillary number (C_{a}):

$$C_a = {}^{\sigma R}\!/_{\gamma_{12}} \tag{3}$$

which represents the ratio between the local acting shear stress σ, that tends to deform the particle and the interfacial stress, γ_{12}/R, that resists to the deformation and tends to restore the initial shape of the particle. Where, R is the droplet radius and γ_{12} is the interfacial tension. R can be calculated through the equation proposed by Tokita: [35]

$$R = \frac{12\alpha\gamma_{12}\phi_{\mathrm{d}}}{\eta_{\mathrm{m}}\dot{\gamma}\pi - 4\alpha\phi_{\mathrm{d}}E_{\mathrm{dk}}} \tag{4}$$

Where ϕ_d is the volume fraction of the dispersed phase; α is the coalescence probability, $\dot{\gamma}$ is the shear rate, and E_{dk} is the break-up energy of the particle. And γ_{12} can be calculated through the method proposed by Wu [36].

To see the effect of the deformation of the dispersed phase on the phase morphology of PS/elastomer blends, other two kinds of elastomer were used to make the blends. One is styrene-butadiene-styrene (SBS) with linear structure, and the other one is SEBS (602) with star structure. The morphology of these blends (80/20) were studied via SEM and the results are shown in Fig. 7, for both static and dynamic samples. It can be observed that, in the PS/SBS and PS/SEBS (star) blends, the dispersed phases have smaller size, and the size of dispersed particles is about 0.2 µm. However, the dispersed phases in the PS/SEBS (linear) have the size about 1.0 µm. These results suggest that the dispersion of elastomer particles is related to the type of elastomers. In fact, all the three elastomers used have polystyrene block, but they have different molecular structures, SBS and SEBS (502) are linear structure, and SEBS (602) is star structure; they also have different molecular weight, as it can be seen from Table 1. So, it can be deduced that the different dispersion of elastomer particles is due to the different molecular structures of elastomers and finally due to the difference of interaction and miscibility between elastomer and PS. When introducing the shear stress into the blends, the role of shear is differ-

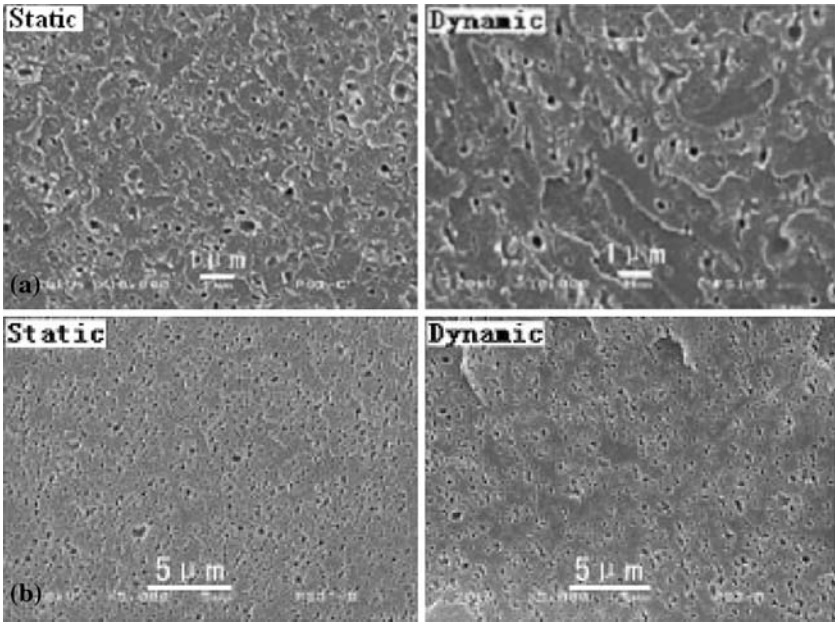

Fig. 7 The morphology comparison between static samples and dynamic samples with the same elastomer content, PS/elastomer = 80/20. (a) PS/SBS and (b) PS/SEBS (star)

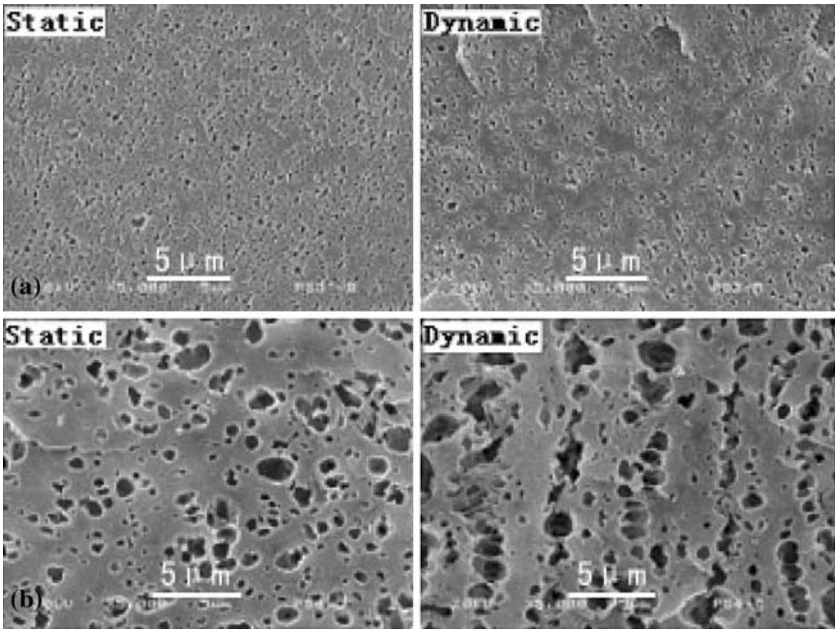

Fig. 8 The morphology comparison of PS/SEBS (70/30) blends between static samples and dynamic samples obtained via the different molding temperature. (a) 180 °C and (b) 210 °C

ent, which can be observed via the SEM results of dynamic samples of different blends. One observes not much morphological change between static and dynamic sample for PS/SBS and PS/SEBS (star) blends, while for the PS/SEBS (linear) blends, the apparent enhanced phase coarsening is observed. Similarly, molding temperature can also affect the viscosity ratio of the blends and finally results in a change of phase morphology. In this work, two different molding temperature (180 and 210 °C) were used to prepare PS/SEBS (linear) blends. And the morphologies of the blend (70/30) obtained at the two molding temperature are shown in Fig. 8. For the static samples, it can be seen that at the lower molding temperature (180 °C), elastomer particles are uniformly dispersed in the matrix and the size is relatively small. While for the blends obtained at higher molding temperature (210 °C), the dispersion of elastomer particles is poor and the size is big. After introducing the shear stress filed, one sees a much enhanced phase coarsening for the sample obtained at 210 °C than that obtained at 180 °C.

The result indeed suggests that dispersed particles with big size can be easily deformed under shear and then shear-induced phase coarsening can be observed. In other words, for blends with much smaller dispersed particles, it is difficult to see the shear-induced phase coarsening. According to the Eq. (3), the bigger the particle size, and the greater the tendency to deform. On the other hand, the greater the shear stress, the easier the deforming, and the greater the interfacial tension, the more difficult to deform. So under the combining effect of shear stress, the deformation of particle increases with the increasing of the elastomer content. This also explains why one observes obvious shear-induced phase coarsening at a higher SEBS content in Fig. 1.

Conclusion

In this work, the morphology and mechanical properties of PS/SEBS blends were studied. These blends were obtained via the conventional molding technology and dynamic packing injection molding technology, respectively. The results suggest a shear-induced phase coarsening in the blends, accompanied by a deterioration of mechanical properties. The degree of phase coarsening induced via shear stress is determined by many factors, such as the elastomer type, elastomer content, and molding temperature. Annealing experiment can be used to diminish the effect of shear stress on phase morphology, and the dispersed particles go back to the small size with spherical and homogeneous distribution.

Acknowledgement We would like to express our sincere thanks to National Natural Science Foundation of China (20274028, 50373030 and 20490220) for Financial Support. This work is also partly supported by Ministry of Education of China for Doctoral Degree (20020610004).

References

1. Olabisi O, Robeson LM, Shaw MT (1979) Polymer-polymer miscibility. Academic Press, New York
2. Utracki LA (1989) Polymer alloys and blends: Thermodynamics and rheology. Hanser, New York
3. Hashimoto T, Kumaki J, Kawai H (1983) Macromolecules 16:641
4. Snyder HL, Meakin P, Reich S (1983) Macromolecules 16:757
5. Rangel-Nafaile C, Metzner A, Wissburn K (1984) Macromolecules 17:1187
6. Hindawi I, Higgins JS, Weiss RA (1990) Macromolecules 23:670
7. Cheikh L, Malone FB, Winter MF (1988) Macromolecules 21:3532
8. Katsaros FD, Malone MF, Winter HH (1986) Polym Bull 16:83
9. Nakatani AI, Kim H, Takahashi Y (1990) J Chem Phys 93:795
10. Katsaros FD, Malone MF, Winter HH (1989) Polym Eng Sci 29:1434
11. Yui SH, Li H, Inoue T (1998) Polymer 39:5265
12. Okamoto M, Shiomi K, Inoue T (1995) Polymer 36:87
13. Wang Y, Zou H, Fu Q, Zhang G, Shen K, Thomann R (2002) Macromol Rapid Commun 23:749
14. Fernandez ML, Higgins JS, Richardson SM (1995) Polymer 36:931
15. Lyngaae-Jorgensen J, Sondergaard K (1987) Polym Eng Sci 27:344
16. Lyngaae-Jorgensen J, Sondergaard K (1987) Polym Eng Sci 27:351
17. Hindawi I, Higgins JS, Weiss RA (1992) Polymer 33:2522
18. Lei C, Li GX, Yang Q, Chen DH, Jiang SJ (2003) J Polym Sci, Part B, Polym Phys 41:661
19. Francesco P, Mauro A, Elisa P, Francesco C (2002) Polymer 43:3323
20. Allen PS, Bevis MJ, UK Pat. 2,170,140B; Euro. Pat, EPO, 188,120B1; U.S. Pat. 4,925,161 (1986)
21. Allan PS, Bevis MJ, British Patent 2170–140–B
22. Allan PS, Bevis MJ (1987) Plastics Rubber Process Appl 7:3
23. Allan PS, Bevis MJ (1990) Compos Manuf 1:79
24. Kalay G, Allan PS, Bevis MJ (1994) Polymer 35:2480
25. Ogbonna CI, Kalay G, Allan P, Bevis MJ (1995) J Appl Polym Sci 58:2131
26. Kalay G, Zhong Z, Allan P, Bevis MJ (1996) Polymer 37:2077
27. Wang Y, Fu Q, Li QJ, Zhang G, Shen KZ, Wang YZ (2002) J Polym Sci Part B Polym Phys 40:2086
28. Janeschitz-Kriegl H, Eder G (1990) J Macromol Sci-Chem A27:1733
29. Horst R, Wolf BA (1991) Macromolecules 24:2236
30. Horst R, Wolf BA (1992) Macromolecules 25:5291
31. Horst R, Wolf BA (1993) Macromolecules 26:5676
32. Katsaros JD, Malone MF, Winter HH (1989) Polym Bull 29:1434
33. Taylor GI (1934) Proc R Soc Lond, A 146:501
34. Grace HP (1982) Chem Engng Commun 14:225
35. Tokita N (1977) Elastomer Chem Technol 50:292
36. Wu SH (1971) J Polymer Sci Part C 34:19